

Electronic supporting informations:

Synergistic Effects from Graphene and Carbon Nanotubes Enable Ordered Hierarchical Structure Foams with combination of Compressibility, Super-elasticity and Stability, and Their Potential Application as Pressure Sensors

Jun Kuang,^{a,b} Zhaohe Dai,^{a,b} Luqi Liu,^{*a} Zhou Yang,^c Ming Jin,^c Zhong Zhang,^{*a}

^a National Center for Nanoscience and Technology, China, Beijing 100190, China

E-mail: liulq@nanoctr.cn; zhong.zhang@nanoctr.cn

^b University of Chinese Academy of Sciences, Beijing 100049, China

^c School of Materials Science and Engineering, University of Science and Technology of Beijing, Beijing 100083, China

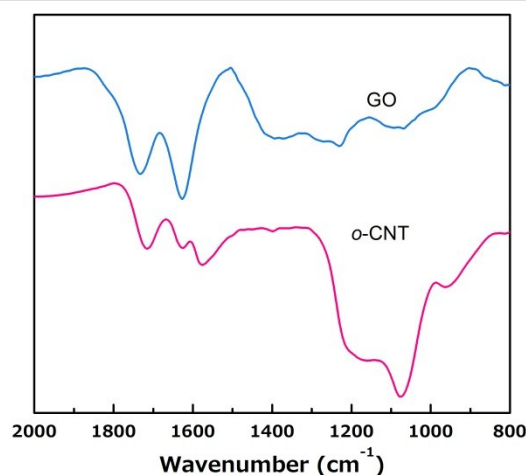


Figure S1. The FTIR spectra of GO (blue line), *o*-CNT (red line).

In the GO curve, the following oxygen contained groups are existed: carbonyl group (1731 cm^{-1}), carboxyl group (1395 cm^{-1}), epoxy group (1228 cm^{-1}), and hydroxyl groups (1074 cm^{-1}); While for *o*-CNT these oxygen contained group are also attached to the CNT: carbonyl group (1714 cm^{-1}) epoxy group (1177 cm^{-1}) and hydroxyl group (1076 cm^{-1}).

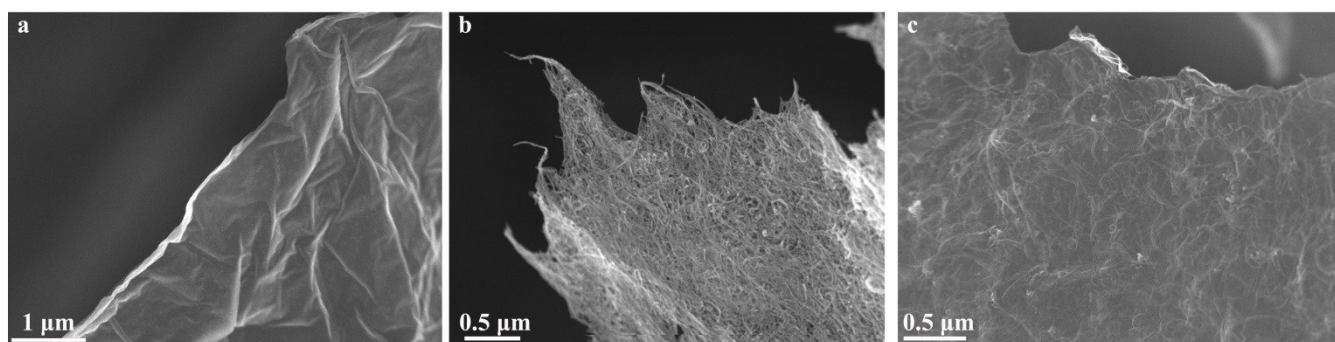


Figure S2. High resolution SEM images of the cell walls. Wrinkled and overlapped graphene sheets in the walls of graphene foam (a); entangled and random distributed CNT in the walls of CNT foam (b); network of CNT covered on the graphene sheets in the hybrid foam (c).

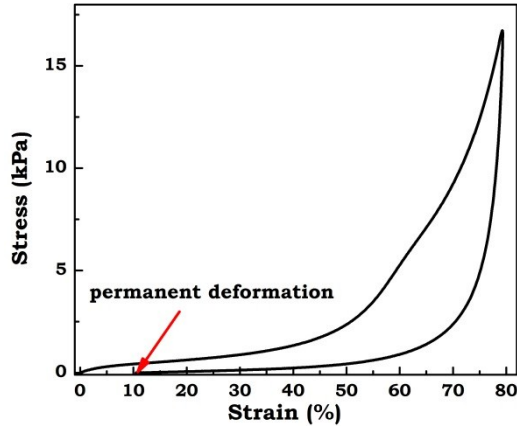


Figure S3. The compressive stress-strain curve of the graphene foam along in plain direction with strain up to 80%. A permanent deformation appeared.

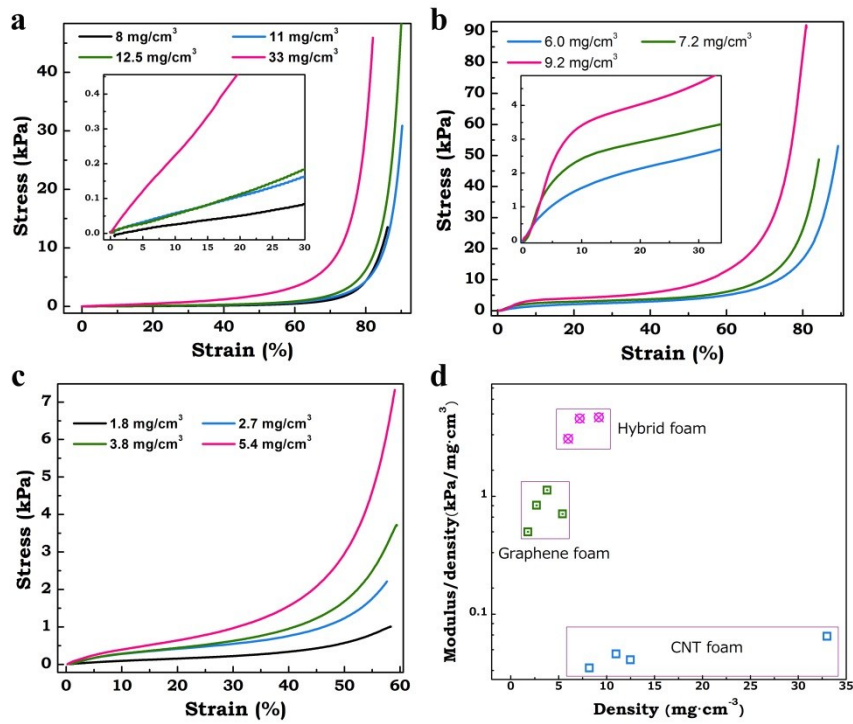


Figure S4. The mechanical properties of CNT, graphene and hybrid foams in different densities are showed in a-c. For comparing their mechanical strength, we list their density eliminated modulus in d.

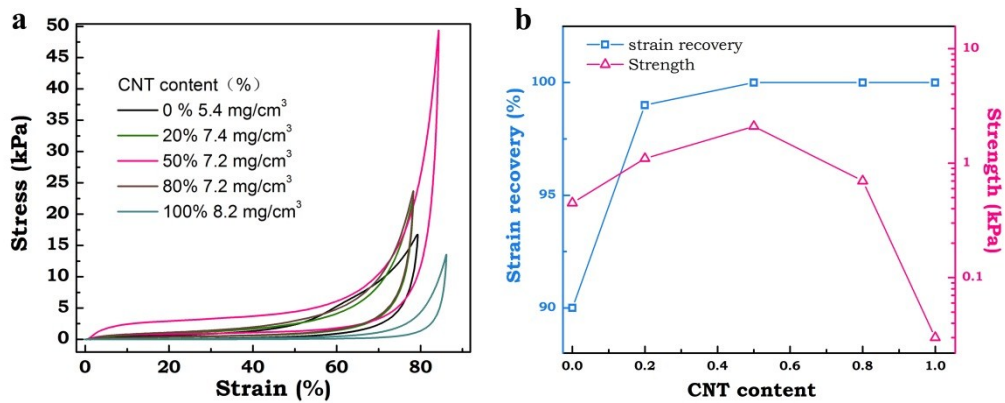


Figure S5. (a) The static mechanical properties of the foams with different graphene to CNT weight ratio. The compression strain was $\geq 80\%$. (b) Strain recovery after removing the compression and the plateau strength of the foams were plotted as a function of CNT weight fraction. Here, the elasticity of the foams were improved with the increasing of CNT content, as the permanent unrecovered strain decreased. The elasticity of the hybrid foam became quite well after the CNT content ratio ≥ 0.2 . However, the plateau strength of the hybrid foams were increased first and then decreased with the increasing ratio of CNT to graphene. And the largest strength of the foam was appeared at the content of 0.5.

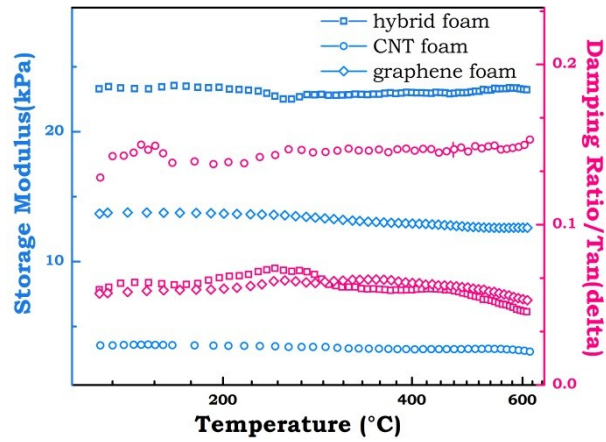


Figure S6. Tests are conducted at -150 - 350 °C, a strain amplitude of 1 %, a test frequency of 1 Hz, Square: hybrid foam, circle: CNT foam and rhombus: graphene foam.

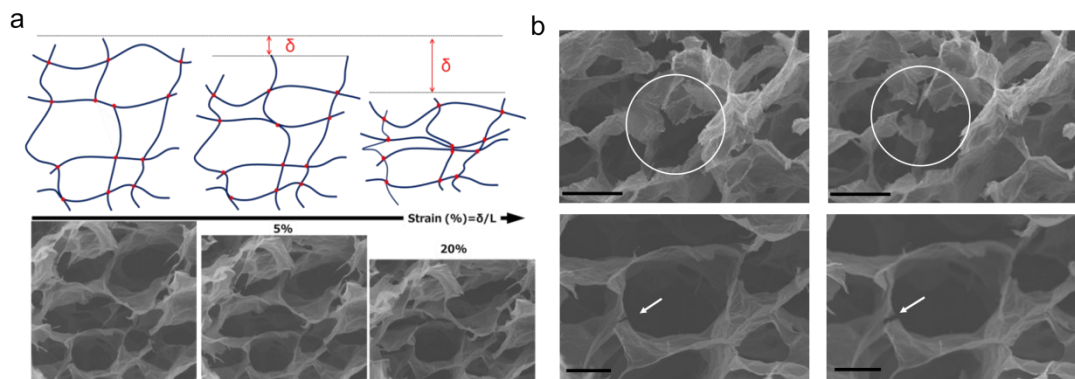


Figure S7. (a). Schematic description and SEM images of the unit cell model of the graphene foam and the evolution in cell structure with strain. The deformation of the cells in the graphene foam is asymmetrical which leading to heavy compression at a local position. (b). SEM images exhibit the variation of the cracks before and after compression to 60%. The cracks propagation would partially or whole broken the cell walls. scale bar: $20\mu\text{m}$ in the upper two pictures and $10\mu\text{m}$ in the bottom pictures in b.

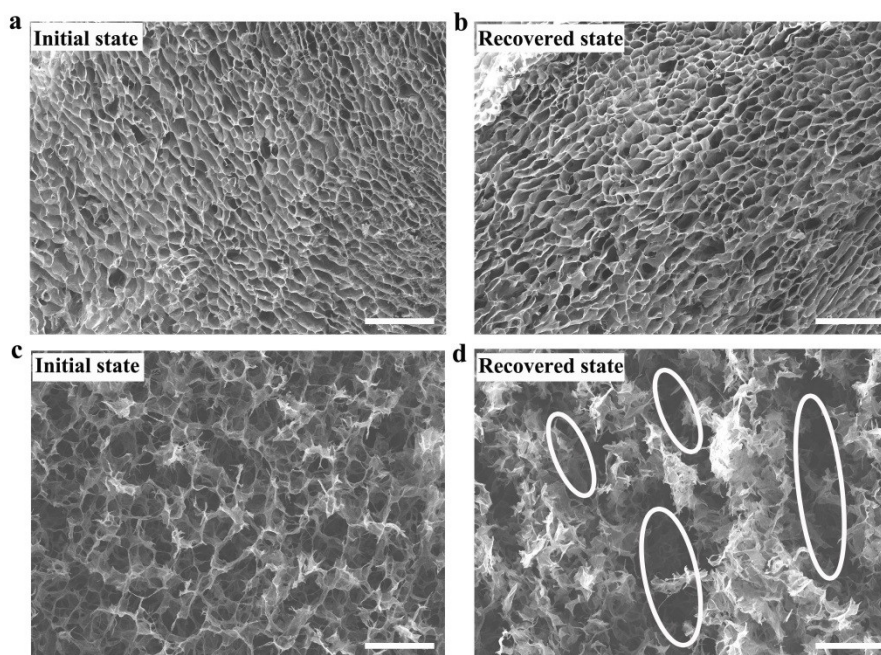


Figure S8. SEM images show the morphologies of hybrid foam (a,b) and graphene foam (c,d), before (a,c) and after (b,d) compressed to 90%. It illustrated that the hybrid foam have good structure stability, no obvious defects were observed in the image after compressed to 90%, while graphene foam can not hold their structure integrity as lots of cracks have been formed after the heavily compression (as white region shown). Scale bar :100 μm .

Table S1. Summary of performance of flexible pressure sensors reported up to now.

	Pressure range (kPa)	Sensitivity (kPa ⁻¹)	Detection limit	Sensor type
CNT/PDMS sponge¹	0-200	0.023	-	Resistance
CB/PDMS sponge ²	0-200	0.046	-	Resistance
Pattern PDMS³	0-10	0.55 (<2 kPa) 0.15 (> 2 kPa)	3 Pa	Organic field-effect transistors (OFET)
Pattern PDMS ⁴	0-20	8.4 (< 3 kPa)	-	OFET
Pattern PDMS⁵	0-10	10.3 (< 3.6 kPa)	27 Pa	Resistance
Pentacene-based sensor ⁶	0-20	0.05	2.5 kPa	OFET
PU foam coated with graphene⁷	0-10	0.26(< 3 kPa)	9 Pa	Resistance
CNT/PDMS ⁸	0-1000	2.3×10 ⁻⁴	50 kPa	Capacitance
ZnO-based sensor⁹	0-30	0.02	3.5 kPa	Piezoelectric
Pt-coated polymer nanofiber ¹⁰	0-1.5	0.15	3 Pa	Resistance
Silk molded CNT¹¹	0-1.2	1.8 (<0.3 kPa)	0.6 Pa	Resistance
Our work	0-13	0.19 (< 2.5 kPa) 0.02 (>2.5 kPa)	36 Pa	Resistance

References

1. J.-W. Han, B. Kim, J. Li, M. Meyyappan, *Appl. Phys. Lett.* **2013**, *102*, 051903.
2. M. G. King, A. J. Baragwanath, M. C. Rosamond, D. Wood, A. J. Gallant, *Procedia Chemistry* **2009**, *1*, 568-571.
3. S. C. B. Mannsfeld, B. C. K. Tee, R. M. Stoltenberg, C. V. H. H. Chen, S. Barman, B. V. O. Muir, A. N. Sokolov, C. Reese, Z. Bao, *Nat. Mater.* **2010**, *9*, 859-864.

4. G. Schwartz, B. C. K. Tee, J. Mei, A. L. Appleton, D. H. Kim, H. Wang, Z. Bao, , *Nat. Commun.* **2013**, *4*, 1859.
5. C.-L. Choong, M.-B. Shim, B.-S. Lee, S. Jeon, D.-S. Ko, T.-H. Kang, J. Bae, S. H. Lee, K.-E. Byun, J. Im, Y. J. Jeong, C. E. Park, J.-J. Park, U. I., Chung, *Adv. Mater.* **2014**, *26*, 3451-3458.
6. I. Manunza, A. Sulis, A. Bonfiglio, *Appl. Phys. Lett.* **2006**, *89*, 143502.
7. H. B. Yao, J. Ge, C. F. Wang, X. Wang, W. Hu, Z. J. Zheng, Y. Ni, S. H. Yu, *Adv. Mater.* **2013**, *25*, 6692.
8. D. J. Lipomi, M. Vosgueritchian, B. C. K. Tee, S. L. Hellstrom, J. A. Lee, C. H. Fox, Z. Bao, *Nat. Nanotechnol.* **2011**, *6*, 788-792.
9. W. Wu, X. Wen, Z. L. Wang, *Science* **2013**, *340*, 952-957.
10. C. Pang, G.-Y. Lee, T.-i. Kim, S. M. Kim, H. N. Kim, S.-H. Ahn, K.-Y. Suh, *Nat. Mater.* **2012**, *11*, 795-801.
11. X. Wang, Y. Gu, Z. Xiong, Z. Cui, T. Zhang, *Adv. Mater.* **2014**, *26*, 1336-1342.